An Operational Framework for Reconstructing Lane-Level Road Maps Using Open Access Data

Cancan Yang, Ling Jiang, Wen Dai, Daoli Peng, Kai Deng, Mingwei Zhao, Xiaoli Huang, and Xi Chen

***Abstract*—Lane-level road maps are crucial for urban traffic management, autonomous driving, and vehicle navigations. Optical remote sensing image suffers from trees and buildings occlusion for lane-level road mapping due to the top-down view. While street view images (SVIs) have been used for road detection, however, most of the previous articles focused on extracting road in image space. The reconstruction of lane-level road maps with measurability in geographic space remains challenging. Hence, this article proposed an operational framework for extracting and reconstructing lane-level road maps from urban open access data. First, a sample strategy was used to collect SVIs based on OpenStreetMap (OSM) road central lines. Then, a deep-learning-based method was adopted to identify lanes accurately, and road width was extracted based on design knowledge and OSM information. Finally, the lane-level road map was reconstructed by integrating the lane and its width information. The proposed framework achieves the transformation from image space to geographic space. The case study shows that 82.43% of the roadway is accurately reconstructed in lane-level. The difference between the reconstructed width of the roadway and the reference true value is within the m-level and the RMSE is 0.32 m. The proposed method is cost-effective and accurate-acceptable for acquiring lane-level road datasets in cities.**

***Index Terms*—Deep learning (DL), open access data (OAD), street view image (SVI), urban road, width measurement.**

Manuscript received 2 March 2023; revised 5 June 2023; accepted 7 July 2023. Date of publication 19 July 2023; date of current version 27 July 2023. This work was supported in part by the Natural Science Foundation of China under Grant 42101425, in part by the Academic Foundation for Top Talents in Disciplines of Anhui Universities under Grant gxbjZD2022069, in part by the Innovation Program for Returned Overseas Chinese Scholars of Anhui Province under Grant 2021LCX014, in part by the Project of Natural Science Research of An-hui Provincial Department of Education under Grant 2022AH040156, Grant 2022AH040150, Grant 2022AH030112, and Grant KJ2020A0721, in part by the Foundation of Anhui Province Key Laboratory of Physical Geographic Environment under Grant 2022PGE013, and in part by the Natural Science Foundation of Chuzhou University under Grant 2022XJYB02. *(Corresponding author: Ling Jiang.)*

Cancan Yang is with the Anhui Province Key Laboratory of Physical Geographic Environment, Chuzhou University, Chuzhou 239000, China, and also with the State Forestry and Grassland Administration Key Laboratory of Forest Resources & Environmental Management, Beijing Forestry University, Beijing 100083, China (e-mail: yangcancan@bjfu.edu.cn).

Ling Jiang, Kai Deng, Mingwei Zhao, Xiaoli Huang, and Xi Chen are with the Anhui Province Key Laboratory of Physical Geographic Environment, Chuzhou University, Chuzhou 239000, China (e-mail: ling.jiang@chzu.edu.cn; dengkai@chzu.edu.cn; zhaomw@lreis.ac.cn; xiaoliray@163.com; chenxi@chzu.edu.cn).

Wen Dai is with the Nanjing University of Information Science and Technology, Nanjing 210000, China (e-mail: wen.dai@nuist.edu.cn).

Daoli Peng is with the State Forestry and Grassland Administration Key Laboratory of Forest Resources & Environmental Management, Beijing Forestry University, Beijing 100083, China (e-mail: dlpeng@bjfu.edu.cn).

Digital Object Identifier 10.1109/JSTARS.2023.3296957

I. Introduction

URBAN road features include urban road geometry, attribute characteristics, and semantic descriptions. The high-precision and rapid extraction of urban road features can provide a data basis for traffic management [1], urban flood simulation [2], urban terrain modeling [3], and autonomous driving [4].

According to Code for design of urban road engineering [5] and literature [3] and [6], urban roads possess the characteristics of direction, grade, and layout. Direction refers to the longitudinal and horizontal directions, while grade signifies the functional classification of urban roads into trunk, primary, secondary, and tertiary (or branch) categories. Layout encompasses various urban road configurations, including single- to four-frame layouts, as well as other specialized arrangements. Urban road is not only the interweaving of line and surface structure, but also the consolidate of various geometric forms. They serve as both receivers and connectors for different physical objects within the urban terrain. Due to the complexity and importance of urban road, studies had attempted to extract urban road feature from different aspect, such as road surface or road boundaries [7], [8], [9], road centerlines [10], [11], [12], and road markings [13].

The advantages of optical remote sensing (ORS) data lie in their macroscopic, multisource, real-time, and massive characteristics [14], [15], [16], [17]. The spectral, geometric, and textural information provided can be used for fine interpretation and extraction of road targets [18], [19], [20]. Therefore, the researches on road extraction methods based on ORS data, especially high or ultra-high-resolution remote sensing data or unmanned aerial vehicle (UAV) images, are very active [19], [21], [22]. Road extraction methods based on ORS images have gone through pixel-based to object-oriented methods and then to deep-learning (DL) methods. The pixel-based methods include spectral analysis [11], threshold segmentation [23], edge detection [24], etc. The object-oriented methods comprise support vector machine, affiliation function, region segmentation, and knowledge model [18], [25], [26], [27]. The DL revolution has had remarkable achievements in the field of computer vision and artificial intelligence in recent years. DL-based methods have increasingly attracted considerable attention in road extraction, such as convolutional neural network (CNN)-based [28], [29], fully convolutional network based [30], generative adversarial network based [31], attention mechanism [32], and edge-detection-based [33] methods. Their optimization model also has achieved high accuracy, efficiency, and robustness for road information extraction [34], [35],

[36], [37], [38]. However, vegetation and building occlusions inevitably exist in road areas in ORS images, which reduce the performance of ORS image-based road surface extraction and yield incomplete results.

As open access data (OAD), street view images (SVIs) present lateral view of urban road, providing a promising and low-cost alternative for overcoming the issues of building and vegetation occlusions. Scholars have attempted to identify road surfaces [39], [40], road centerlines [41], [42], and traffic marking lines [43], [44], [45] from SVIs. The methods could be categorized into two types: feature engineering and DL-based methods. Feature engineering methods use various computer vision operators to extract relevant ground lane lines for identification and reconstruction of road network [46], [47], [48], [49]. DL-based methods have recently shown a superior performance in lane detection. The main methods include semantic segmentation, row classification, and anchor-based detection. The semantic segmentation method classifies all pixel points that correspond to roads in an image [50], [51]. Row classification divides SVI images into equal distances in row direction; and then identifies the marking lines in each row [52], [53]. The anchor-based detection creates the lane lines as rays from starting points (left, bottom, and right) to numerous horizontal deviation points (offsets), and then fits the actual lane lines [54]. The DL-based method can easily identify and segment road objects from SVIs. However, the road detection of these methods remains confined to the image space with side-view, which is difficult to reconstruct high-precision (lane-level) road maps with measurability and limits its directly application further. This is because the perspective transformation from lateral view into measurable planar view is complex and difficult [55], [56]. Therefore, reconstructing measurable lane-level road maps from SVIs remains challenging.

In addition to the SVIs, the OpenStreetMap (OSM) is a common and freely available road network data source, which contains rich information of urban roads (e.g., road names and road grades). Through the evaluation of OSM data, researchers have consistently held a positive attitude to OSM, considering it one of the most complete sources of global transportation data and marking a new age of geographic information [57], [58], [59], [60]. It is widely used in urban and road related field [61], [62], [63], [64]. OSM provides geolocation of the road central lines, but lacks the number of lane and width information. Meanwhile, SVIs offer a detailed view of urban roads making it suitable for road features identification and extraction, which potentially provides the lane and width information. Combining OSM and SVI is promising for reconstructing measurable lane-level road maps, while solving the inaccessibility problem of non-OAD. However, the gaps to reconstructing geospatial measurable lane-level road maps from OSM and SVIs still exist: 1) road width cannot be directly measured from SVIs due to the complex perspective transformation; and 2) SVI and OSM data are different in sources and geometric types but should be matched for road reconstruction.

To address the challenges mentioned above, the article proposed a novel operational framework. The main contribution of this article is presented as follows.

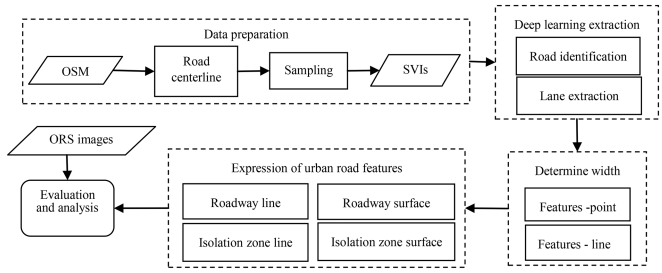

Fig. 1. Flowchart of the proposed approach.

1) A U-OAD-based reconstruction operational framework for lane-level road map, which provides a new insight into the transformation of side-view image information into geospatial data, was proposed.
2) The DL-based method and road design knowledge were integrated in the operational framework for road reconstruction. The DL-based method was adopted to identify lanes accurately, road design knowledge, and OSM information were then used for road width reconstruction.
3) A set of approaches was raised for workflow optimization. A sampling strategy was conducted for collecting SVIs. The road reconstruction results were optimized by a majority vote approach.

The rest of the article is organized as follows. Data and methods are described in Section II. Section III provides the experimental results and analysis, followed by discussion of the method, data sources, and deficiencies in Section IV. Finally, Section V concludes this article.

II. Materials and Methods

A. Basic Idea

Urban road, especially double-layout road and above, consists of roadway for vehicle, median strip, cycle lane for bike or e-bike, separation belt between roadway and cycle lane, nature strip, sidewalk, etc. [3], [5], [6]. To simplify the article's aim, this article only focuses on lane-level roadway for vehicle. The one-way roads in the experimental area are divided into the following four types in this article: single lane, dual lanes, three lanes, and four lanes or more. If a gap exists between the positive and negative driving directions, then this gap is the area of the separation facilities, such as median strip, separation belt, and nature strip, which are defined in this article as the isolation zone. Fig. 1 shows the technical route. First, the centerline of the road is extracted from the vector road network data, and the sampling method is carried out along the road center line. Second, the DL method is used to identify the road and the number of lanes on the roadway based on the acquired SVIs. The width at the sampling point is then determined in accordance with the road measurement specification and the road grade. The remote sensing image is used to evaluate the accuracy of road width, and the roadway is finally constructed and expressed.

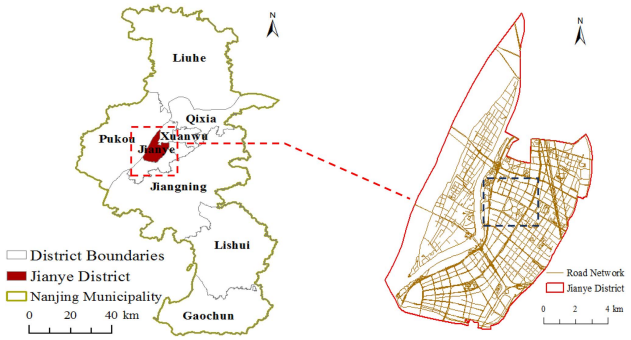

Fig. 2. Experimental area (black dashed box) and urban road network.

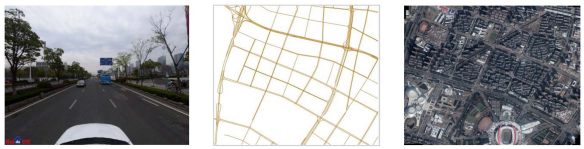

Fig. 3. Experimental data. (a) Street view image. (b) Road network. (c) Remote sensing image.

B. Experimental Areas and Data

1) Experimental Areas: The Jianye District of Nanjing City is taken as the experimental area in this article. This District is located in the middle of the main city of Nanjing, covering an area of approximately 81 km^2. The traffic is well developed within the experimental area. This area has roads with trunks (such as Yingtian Street, Yangzijiang Avenue, and Nanjing Ring Expressway), primary roads (such as Shuiximen Street, Jiangdong Middle Road, and Olympic Street), secondary roads (for instance, Changhong Road and Fuchunjiang West Street), and branch roads (Mochou Lake East Road, Memorial Hall East Road, etc.) (Fig. 2). Road types are rich and roadway features are well displayed. It is a good representation of the roads in the whole city.

2) Data and Preprocessing: The experimental data include SVIs, road network, and remote sensing images, as shown in Fig. 3. The road network was obtained from the OSM platform, and the residential area roads were eliminated on the basis of attribute information and geometric correction was made. The SVIs were downloaded by using Baidu URL according to the set coordinates of sampling points. The height and width of the SVI are 480 and 640 pixels, respectively, and the vertical angle of view at each sampling point is 0°. Meanwhile, the horizontal angle of view starts from 0°, and the heading value is consistent with the road direction. The remote sensing images are used for geometric correction of road centerline and reference for accuracy evaluation of road width. The images come from the Google Earth, with a resolution of 0.2 m, including the red green blue bands.

C. Road Centerline and Sample Setting

The road network of the OSM presents the "one to many" characteristic, that is, one road with the same road name corresponds to multiple road lines, especially high-level roads. The setting of the original road centerline is retained in this article because of the following two advantages: 1) the convenience of knowing the vehicle lane and its attributes of one- or two-way driving as mentioned above; and 2) it facilitates the identification of isolation zone (the gap between the lane surface of the two-way road).

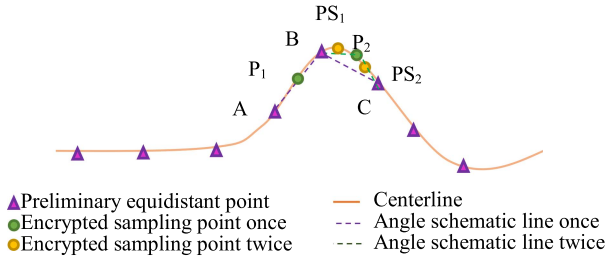

Fig. 4. Sampling approach of urban roads.

The article proposes a sampling method based on the characteristics of road features, which were divided into two parts: equal distance sampling and special feature sampling. According to [65] and [66] and considering efficiency, the road network was sampled equidistant along the central line with 100 m distances, and then, the sampling points in curved road section were densified (Fig. 4). The densified treatment process was outlined as follows.

1) The angle value between two line-segments comprising the current and the front and rear sampling points, such as $\angle ABC$, is determined. If the value is less than the angle threshold value ∂, then step (2) is executed; otherwise, no special treatment is required.
2) One point in the middle is added between the current and the previous and the latter sampling points, such as $P1$, $P2$.
3) The newly added point is taken as the current point, and the included angle with the front and rear sampling points is redetermined. If the angle is less than ∂, then step (2) is repeated; otherwise, step (4) is performed.
4) If all the included angles are larger than ∂, then the densified treatment of the sampling points in the curved road section is completed. The angle threshold value ∂ is set to 150° in this article based on experiments and literature [5].

D. Measurement of Road Width

1) Identifying Lanes: Reconstruction of roadway from centerlines of OSM requires road width measurement. The article presents an approach inferring road width from SVIs. An urban roadway generally comprises several lanes, and the lanes have fixed width according to certain standards. If the number of lanes is known, then the road width can be calculated. Hence, a neural network is initially used for identifying lanes from SVIs, and the road width is then reconstructed on the basis of the number of lanes.

The determination of lane number is a typical segmentation problem in computer vision. The Mask R-CNN based on the ResNet101 architecture [67], [68] is the classic segmentation

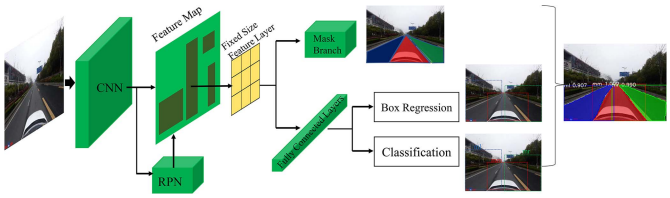

Fig. 5. Structure of Mask R-CNN.

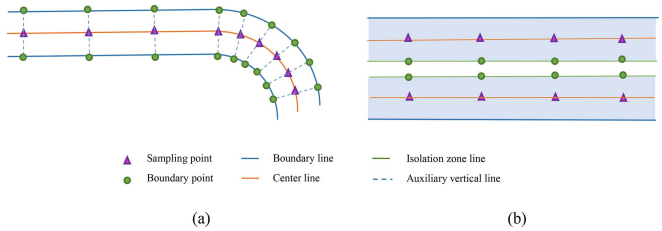

Fig. 6. Road features construction and expression. (a) Generation of road boundary. (b) Road surface and spatial relationship.

network, which combines object detection and semantic segmentation to achieve lane segmentation. The network can detect different lane surfaces from the same road. Fig. 5 shows the network structure of Mask R-CNN. More than 1500 street scene images were randomly selected in the study area and manually labeled with road lanes to train the neural network. A total of 665 images were then used to validate the performance.

The trained Mask R-CNN returns the labels of lanes in an SVI. To reconstruct the width of road, the number of labels (lanes) must be counted and then converted to width. A large number of SVIs exist, thus a batch procedure was designed to extract the number of lanes. First, the batch procedure takes out the photos from the identified folder of SVIs and records the photo ID, longitude, and latitude to a table. Second, the SVIs were inputted into the trained Mask R-CNN network and the number of the labels (lanes) was then counted for each street scene image according to the predicted images of Mask R-CNN.

2) Reconstructing Road Width: According to [5], the lane width of main roads (inter district) and general roads (within district) in China are 3.75 and 3.5 m, respectively. The main and general roads were classified in the article according to the OSM information. Besides the land width, another problem should also be addressed: the incorrect identification of lanes from SVIs would exist in the same road. That is, although the road width is fixed, a part of the roadway may be recognized as three lanes and another part may be four lanes due to quality differences of street scene images. Therefore, the majority voting method was introduced to determine the number of lanes within the same road. For example, if the number of images with three lanes is more than that of four lanes, then the road will be determined as a three-lane road. If an anomaly was found after majority voting, it will be checked manually and SVIs with better quality will be reacquired near the original sampling point. The road width was finally determined by the lane width and the number of lanes.

E. Road Construction and Expression

The idea of "from point to line, convert line to surface" was adopted in the article to generate roadway based on road sampling points. Urban road boundary was generated by boundary fitting method considering road bidirectional constraints. That is, the longitudinal extension direction of roads is controlled by road center line, while the road cross-section boundary is fitted by edge line on the basis of obtained boundary coordinate points. Fig. 6 shows the generation process of the urban road boundary lines as follows.

1) The ownership relationship between the sampling point and centerline was established by using the principle of the shortest distance.
2) The road transverse auxiliary line was generated by taking the current sampling point as a reference, that is, the line segment perpendicular to the road centerline.
3) The obtained road width was transformed into a boundary coordinate point along the vertical direction, that point is called the boundary point for short.
4) The boundary points of different types of road sections were fitted in sections.

F. Accuracy Assessment

The accuracy assessment in this article involves the following three aspects: the accuracy of lane identification from SVIs, the accuracy of identified lane number of roads, and the accuracy of reconstructed road width. The manual interpretation of lanes from SVIs was used for comparison with the lane identification results. If the identified number of lanes is equal to that of manual interpretation, then it is regarded as correct identification. The correctness index was designed to evaluate the performance of lane identification

$$\text{correctness} = (Nt/Ns) * 100\% \tag{1}$$

where *Nt* represents the number of SVIs with correctly identified numbers of lanes and *Ns* represents the number of all SVIs. The correctness was also used for quantifying the accuracy of identified lane number of roads. Therefore, the *Nt* represents the number of correct identification roads (the number of their lanes is equal to that of manual interpretation), and the *Ns* represents the number of all roads in the study area.

The Bias, MAE, R^2, RMSE, and Std were adopted as, respectively, shown as follows to estimate the accuracy of reconstructed road widths:

$$\text{Bias} = \frac{1}{n} \cdot \sum_{i=1}^{n} (x_i - y_i) \tag{2}$$

$$\text{MAE} = \frac{1}{n} \cdot \sum_{i=1}^{n} |x_i - y_i| \tag{3}$$

$$R^2 = 1 - \frac{\sum_{i=1}^{n} (x_i - y_i)^2}{\sum_{i=1}^{n} (x_i - \bar{y})^2} \tag{4}$$

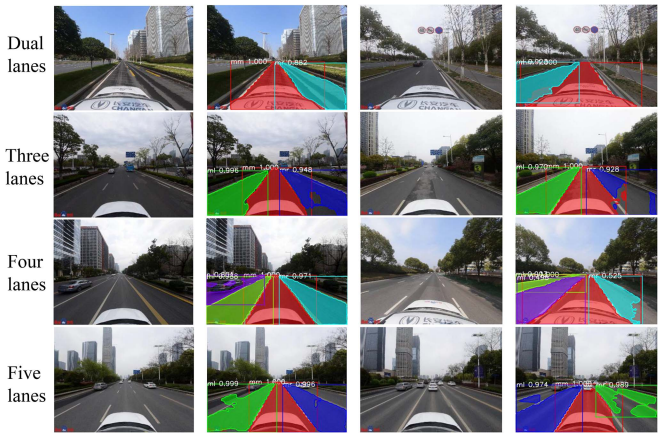

Fig. 7. Identification results of lane number in street view.

TABLE I
ACCURACY ASSESSMENT OF DIFFERENT TYPES OF ROADS

	SVIs			**Roads**		
	Nt	*Ns*	Correctness	*Nt*	*Ns*	Correctness
Dual lanes	285	328	86.89%	63	64	98.44%
Three lanes	176	247	71.26%	57	62	91.94%
Four or more lanes	21	77	27.27%	2	22	9.09%
All data	482	652	73.93%	122	148	82.43%

$$\mathrm{RMSE} = \sqrt{\frac{1}{n} \cdot \sum_{i=1}^{n} (x_i - y_i)^2} \tag{5}$$

$$\mathrm{Std} = \sqrt{\frac{\sum_{i=1}^{n} (x_i - \bar{x})^2}{n-1}} \tag{6}$$

where x represents the width measured by this method at the test point, and y represents the reference true value at this location, where the reference data were obtained by measuring the one-way road width of the unoccluded and uncovered area in the orthoimage. $\bar{x}$ and $\bar{y}$ represent the average of x and y, respectively.

III. RESULTS

A. Identification of Lanes

Fig. 7 shows the results of identifying lanes from SVIs by Mask R-CNN. Oversegmentation and undersegmentation could be found in several images (Fig. 7). However, it only has a minor effect on the identified number of lanes. There are 652 photos in the experimental area, and the number of lanes was correctly identified in 482 SVIs. The correctness is 73.93% according to (1). Further analysis of accuracies in different types of roads was conducted. Table I shows that the Mask R-CNN has different performances on various types of roads. The correctness is 86.89% and 71.26% in the dual- and three-lanes images, respectively, but substantially low in four or more lane images (only 27.27%). Single lanes are recognized with high accuracy, but there are no single lanes in key areas. If four or more lanes are existed, the lanes on the extreme sides are very narrow (four and five lanes in Fig. 7) in SVIs due to the perspective transformation of street view cameras. This phenomenon leads to the misidentification of lanes on the extreme sides.

To avoid the impact of misidentification in some images on road widths, majority voting was conducted to determine the number of lanes for a one-way road after identifying the number of lanes from the SVIs. A total of 148 roads in the sample area (one-way statistics) are analyzed statistically, and the identification results are shown in Table I. The number of 122 roads were correctly identified, and the correctness value is 82.43%. This result shows that majority voting reduces the impact of misidentification in SVIs, especially for dual- and three-lanes roads. However, the correctness of roads with four of more lanes is still low. Because several four or more lane roads were disregarded as three-lane roads (Fig. 7), the vote of three-lanes would be higher than that of four-lanes during mode voting, resulting in misidentification of the lane number of roads. This misidentification is a limitation of the Mask R-CNN and majority voting method.

B. Reconstruction of Roads and Accuracy

The identified number of lanes was converted into road widths based on the standard width of lanes. The roadway surfaces were reconstructed by the method in Section II-E according to the obtained urban road center line and the corresponding width information. The reconstructed roadway has geometric and spatial information including road direction, length, and width. The results are shown in Fig. 8 combined with the remote sensing image, in which blue represents the polygon of roadway and orange represents center line. The isolated zone (the gap) in the middle between motorways is expressed in green color for easy observation and comparison. The right is a partial enlargement of the red box area on the left [Fig. 8(a) to (f)].

The results reveal that this method can reconstruct the roadway of urban and isolated zone, which are in good agreement with the remote sensing image. Fig. 8(a), (b), (c), (e), and (f) shows many vegetation or building shadows or covered areas, which can substantially affect the road extraction effect. However, the extraction results in this article are not affected by the aforementioned condition thereby demonstrating correct reconstruction. Fig. 8(b) shows a road without median strip. Simultaneously, the width of the reconstructed roadway is wider than that of the exposed roadway in the image, indicating that the proposed method can effectively identify the roadway boundary under the street tree. Fig. 8(a) to (f) shows the reconstruction results of roadway with different numbers of lanes and layouts. Meanwhile, Fig. 8(h) to (i) shows the reconstruction results at complex intersections and road links. The figures reveal that the reconstruction results of the proposed method can be successfully integrated with the image, and the curve of the road can also be effectively expressed. However, the roadway surface depends on the establishment of the center line, thus, the part of the center zone intersection is missing and has not been further refined [Fig. 8(e) and (h)].

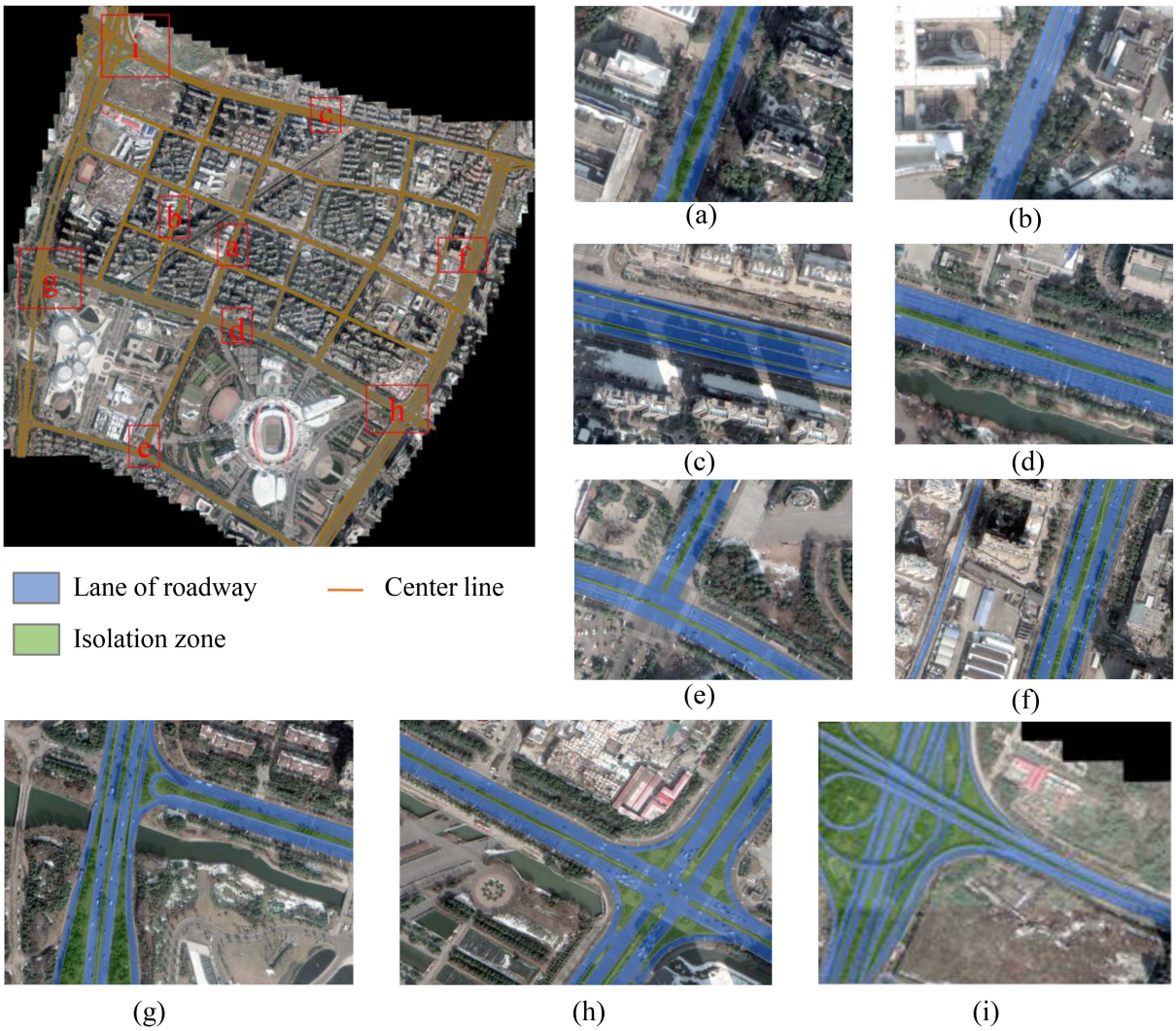

Fig. 8. Reconstruction results.

The measured width from orthographic remote sensing images (Width-IM) was taken as the reference truth value for width accuracy assessment of the reconstructed road based on street view acquisition (Width-SVI). Since this article only conducted experiments on the roadway, attention should be paid to the measurement of reference images. When measuring the reference boundary, the place without occlusion and the road edge line can be well seen should be selected for measurement, and a total of 176 test points were chosen. Table II shows that the minimum deviation value (DV) of the urban road surface width is 0.01 m, the maximum DV is 0.93 m, the bias is 0.10 m, RMSE is 0.32 m, and the relative error is less than 3%, where DV is computed by subtracting Width-IM from Width-SVI. The RMSE deviation between the plane accuracy of the 1:1000 topographic map data measurements and the adjacent ground feature points shall not be larger than 0.4 m, that is, the field distance is 0.4 m. In addition, the DV values conform to a normal distribution, with 82% of the data concentrated between −0.4 and 0.4 m. The results show that the precision of the urban roadway width measurement based on SVIs can meet the plane precision of the large-scale topographic mapping. The method can effectively measure the width of the urban roadway based on the above analysis.

TABLE II
ERROR STATISTIC OF THE ROAD WIDTH

	|Width-SVI- Width-IM | (m)	Width-SVI- Width-IM (m)
Max	0.93	0.93
Min	0.01	-0.85
Median	0.17	0.11
Std	0.21	0.31
Bias	0.10	
MAE	0.25	
RMSE	0.32	
R^2	0.99	

C. Reconstruction of Isolation Zone and Accuracy

This article takes the gap in the middle of the motor vehicle lane as the isolation zone area, such as median strip or other flower beds. The result can still effectively express the area covered by the isolation zone (Fig. 8). Fig. 8(a), (d), and (e) indicates that the green area is the flower bed between two motorway lanes. There is no obvious blank area in Fig. 8(b), so the road has no isolation zone and only has a line as a marker to distinguish the positive and negative direction of road traffic.

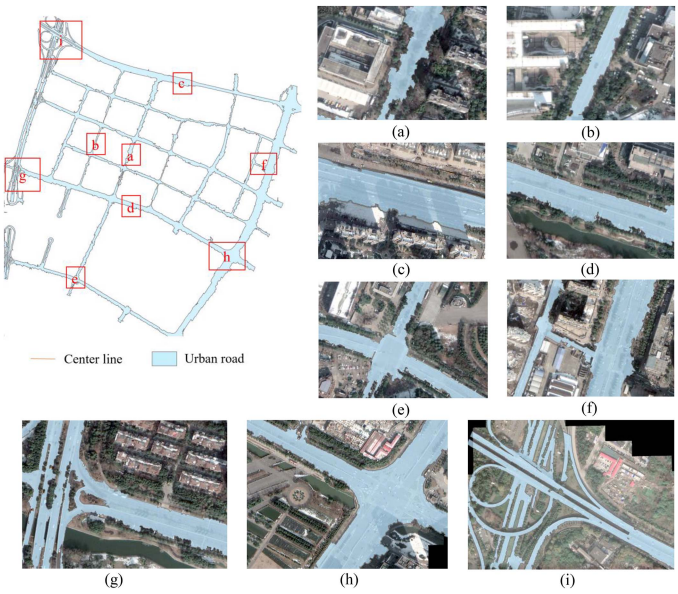

Fig. 9. Urban road extraction by ORS image-based method.

Fig. 8(c) and (e) represents the isolation zone between multiple lanes. The reconstructed isolation zone in this article is in good agreement with the isolated area boundary in remote sensing image. A defect is also observed, that is, the shape of isolation zone, such as flower bed, varies with the shape of the roadway. If the lane is correctly expressed, then the shape of the isolation zone area can also be well expressed, such as traffic island [Fig. 8(g) and (i)]. If the roadway lane has equal width, the isolation zone shows a rectangular geometry [Fig. 8(a), (d), and (e)]. The center of the roadway at the intersection is expressed as the isolation zone [Fig 8(e) and (h)]. Overall, the proposed method in this article can express the roadway and the areas between them.

A total of 20% of the number of roads were randomly selected in this article as the number of verification points. The middle part of the road with stable width of the isolation zone was selected for measurement to avoid the areas where the isolation zone changes at both ends, and the width of the reconstructed isolation zone was compared. Similar to the road width measurement method, the unshielded and clear boundary area is also selected for measurement. Statistically, the RMSE and MAE are 0.64 and 0.41 m, respectively.

IV. Discussion

A. Comparison of Different Methods

To verify the effectiveness of the proposed method in the article that is based on U-OAD, the ORS image-based method [18], [25] was used for comparative experiments. The ORS image-based approach can extract the urban roads with 0.80 Kappa value, however, road breaks, incomplete and not smooth boundaries appeared (Fig. 9). The emergence of these conditions is due to the shadows and occlusions of vegetation and buildings observed from the top-down view of ORS images. For example, the areas shaded by trees in the road are not extracted by ORS image-based method in Fig. 9(b), therefore the width of the extracted road is narrower than the actual road. While the shaded areas of buildings and trees are treated as road surfaces in Fig. 9(c), and road breaks appear at the bottom of Fig. 9(g) and in the middle of Fig. 9(i). Besides, the unroad surface (hardened or impervious surface) next to the road is included [Fig. 9(a), (c), (d), (f), and (i)], mainly due to the same spectrum of foreign matter.

The ORS image-based method focuses on the extraction of the entire road surface and does not differentiate individual lanes, while the proposed method can reconstruct lane-level roadway. In addition, rather than selective extraction (such as primary or secondary road), the ORS image-based method extracts all the roads in the entire experimental area. Meanwhile, the proposed method can extract specific grade road according to the attributes of OSM data. Moreover, the extraction method based on ORS images is markedly affected by the time and phase of data acquisition, and extraction when the vegetation is dense and seriously covered by trees or clouds is difficult. The extraction and reconstruction of urban road in this article is unaffected by the quality of ORS images and can also reduce or eliminate the problems of occlusion and shade from trees or buildings, as well as other impact problems (such as weather and different radiation of road surfaces), due to side-view and close-up photogrammetry and nonspectral information extraction.

Some ORS image-based methods also attempted lane-level road extraction. For example, Dai et al. [69] proposed a high-resolution optical satellite image lane-level road extraction method. The results show that a complete road network can be extracted under interference from buildings, trees, and partial or complete shadows, but the article did not extract road surface. Indeed, the proposed method is superior to these ORS image-based methods.

The surface- and line-based detection methods are widely used in the lane detection from SVIs. The Mask R-CNN was used to identify lane surfaces from SVIs to determine road width. Meanwhile, many articles identify lane lines with a high accuracy based on SVIs, for example Shi et al. [56]. If the lane lines are detected completely, then the number of lanes can also be determined. Thus, given the same data source and road scenarios, the proposed method (surface-based) was also compared with their method (line-based) in Jianye District. Fig. 10 shows the results. The two methods have similar detection performance in single and dual lanes. However, the surface-based method is superior with the increasing number of lanes. In the detection of three or more lanes, the line-based method may lose the outermost lane lines, resulting in lane number misidentification. The surface-based approach identifies only part of the outermost lane rather than all of it, but it does not affect the final result, because only the number of lanes is counted, and the identification of partial lane is acceptable. Further, the final road map results will be more correct, if the accuracy of number of lanes is higher. Thus, the surface-based lane detection method is superior for the workflow of the lane-level road reconstruction.

The proposed method is more flexible in time and space because side-view images are not subject to time and weather. Moreover, the SVIs are also accessible in most of cities. Thus, the proposed method can be easily applied to other cities or

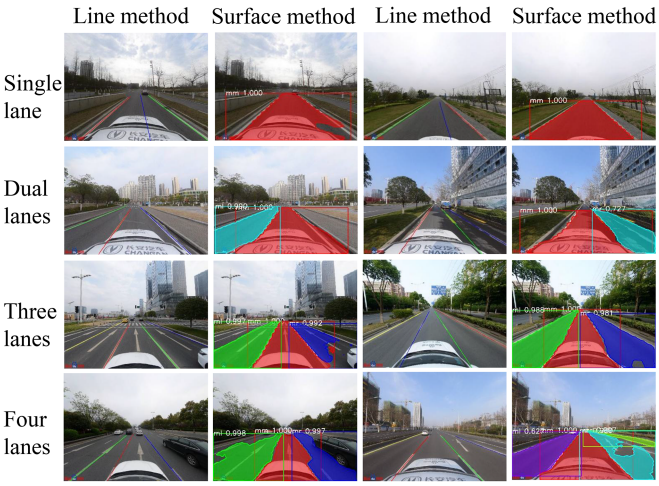

Fig. 10. Comparison of surface-based and line-based method.

provinces. However, attention should be paid to road design rules when applying the method to national-scale. Since the proposed method integrated the DL-based method and road design knowledge (in China) for reconstructing road width. Road design rules may vary in different nation, which could change some of the parameter settings in the proposed framework. Even so the proposed framework can still provide guidance and reference for road reconstruction in various nations. City-level urban road map dataset will be established in follow-up study, so as to provide support for its open source data acquisition application.

B. Urban Road Reconstruction From Multiple Data Sources

Although ORS or UAV images have an important role in urban road element (road boundaries or surfaces) extraction, these images are inadequate and flawed in the previous section. In addition to the SVI data (side view) mentioned in this article, data sources that can overcome the complex scenes of urban roads and are unaffected by shadows and clouds including airborne (handheld) LiDAR [70], [71], vehicle trajectory [72], [73], and digital topographic map data [3], [6]. Airborne or handheld LiDAR data can obtain fine urban road elements, including road edge lines and centerlines, identification lines, and road ridges. However, the data processing and extraction of massive point clouds are still the key problems to be solved and the cost of data acquisition must be considered. The trajectory data are obtained through the GPS on vehicles (such as taxi) to obtain the driving trajectory. The road centerline data can be obtained based on trajectory data. But the road surface mapping is still challenging because vehicles are generally rarely driven along the roadside and the distance error between the location of GPS points and the road boundary is inevitable. Most importantly, the two abovementioned data are usually non-OAD, increasing the difficulty of their application to large areas, which introduces certain challenges to the article. Excluding the data error itself, the road features extracted from large-scale digital topographic maps are relatively comprehensive, and the error is small, but some problems, such as hard data acquisition and a high level of confidentiality, are still encountered [74]. In addition, the multisource fusion and complementary advantages of various data are issues examined by researchers on [10] and [75].

Compared with the original OSM, the essential difference is that the original road network is the skeleton line data, the reconstructed roadway in this article can express the transverse shape, width, position, and other geometric information of the lane surface. Simultaneously, the detailed information, such as road curves, which can be expressed in the original road network can also be obtained by proposed method. In addition, the original skeleton line cannot express the information of the separation belt between the motor vehicle lanes in different directions [Fig. 3(b)]. By contrast, the proposed method can directly or indirectly express the relationship or the position between the separation belt and the lanes surface and other geometric or semantic information (Fig. 8).

Therefore, the OAD used in this article, including SVI and OSM, are relatively economical, easily to obtained, and effectively reconstruct roadway maps. The synergistic use of multisource data should be further considered to form a complementary advantage in the future.

C. Shortcomings and Limitations

Despite the advantages, the accuracy of road reconstruction depends on the quality of OAD. The number of lanes in approximately 26% of the SVIs is still incorrectly recognized, and the higher false recognition rate occurs in the SVIs containing four or more lanes. The possible reasons are that the recognition effect is related to the quality of the SVIs (e.g., lane line clarity and vehicle status on the road), the angle of the SVI acquisition, the road structure (possible presence of median strip), and the model parameters. Simultaneously, the lane line recognition is incomplete in the presence of an excessive number of road lanes and the visually different widths of various roads. This incomplete phenomenon accounts for the majority of the recognition errors. Moreover, the centerline's position and the width's accuracy will affect the road's width. Before road surface reconstruction, the geometric correction of the road centerline is conducted in this article with the remote sensing image as a reference. The error caused by the offset of the centerline is reduced.

The overall width of the road remains fixed, but the geometric width of the motorway and flower bed of the isolation zone is changed [Fig. 8(f) and (h)]. The lane appears to increase at the road intersection [Fig. 8(e) and (h)]. These current conditions increase the difficulty of accurately expressing the roadway. In this article, experiments are conducted under the assumption that the lane width is fixed, and the lane number variation at the intersection is intentionally ignored. The idea of voting and large probability is used to consider the lane width as the normal road width at the nonintersection, thus reducing its complexity.

V. Conclusion

The article proposed an operational framework for extracting and reconstructing lane-level road maps based on U-OAD. The transformation of roadway from image space to geographic

space is realized by comprehensively using DL-based method and road design knowledge. The proposed method correctly identifies 82.43% of the roadway lane numbers of SVIs. The deviation error is within the m-level and the RMSE is 0.32 m. The method proposed in this article can solve the problems of vegetation occlusion and building shading, the uncertainty of the road boundary, with low cost. This article provided an insight for lane-level urban road reconstruction, autonomous driving, and vehicle navigations.

REFERENCES

[1] D. M. González, J. M. B. Morillas, and G. Rey-Gozalo, "Effects of noise on pedestrians in urban environments where road traffic is the main source of sound," *Sci. Total Environ.*, vol. 857, Jan. 2023, Art. no. 159406, doi: 10.1016/j.scitotenv.2022.159406.

[2] H. Zhu, M. Yu, J. Zhu, H. Lu, and R. Cao, "Simulation study on effect of permeable pavement on reducing flood risk of urban runoff," *Int. J. Transp. Sci. Technol.*, vol. 8, no. 4, pp. 373–382, Dec. 2019, doi: 10.1016/j.ijtst.2018.12.001.

[3] C. Yang, M. Zhao, C. Wang, K. Deng, L. Jiang, and Y. Xu, "Urban road DEM construction based on geometric and semantic characteristics," *Earth Sci. Inform.*, vol. 13, pp. 1369–1382, Sep. 2020, doi: 10.1007/s12145-020-00510-4.

[4] K. Jiang, D. Yang, C. Liu, T. Zhang, and Z. Xiao, "A flexible multi-layer map model designed for lane-level route planning in autonomous vehicles," *Engineering*, vol. 5, pp. 305–318, Apr. 2019, doi: 10.1016/j.eng.2018.11.032.

[5] "Code for design of urban road engineering (CJJ/37-2016)," Ministry of Housing and Urban Rural Development, Beijing, China, China Architecture & Building Press, 2016.

[6] Y. Tao, C. Wang, Y. Xu, Z. Zhang, S. Song, and W. Yang, "Classification and expression of urban road from the perspective of DEM modeling," *J. Geo-Inf. Sci.*, vol. 22, no. 8, pp. 1589–1596, Aug. 2020, doi: 10.12082/dqxxkx.2020.200004.

[7] M. Yadav, A. K. Singh, and B. Lohani, "Extraction of road surface from mobile LiDAR data of complex road environment," *Int. J. Remote Sens.*, vol. 38, no. 16, pp. 4645–4672, May 2017, doi: 10.1080/01431161.2017.1320451.

[8] D. Rato and V. Santos, "LIDAR based detection of road boundaries using the density of accumulated point clouds and their gradients," *Robot. Auton. Syst.*, vol. 138, Apr. 2021, Art. no. 103714, doi: 10.1016/j.robot.2020.103714.

[9] W. Yang, T. Ai, and W. Lu, "A method for extracting road boundary information from crowdsourcing vehicle GPS trajectories," *Sensor*, vol. 18, no. 4, pp. 1261–1283, Apr. 2018, doi: 10.3390/s18041261.

[10] Z. Zhang, X. Zhang, Y. Sun, and P. Zhang, "Road centerline extraction from very-high-resolution aerial image and LiDAR data based on road connectivity," *Remote Sens.*, vol. 10, no. 8, pp. 1284–1304, Aug. 2018, doi: 10.3390/rs.10081284.

[11] X. Lu et al., "Cascaded multi-task road extraction network for road surface, centerline, and edge extraction," *IEEE Trans. Geosci. Remote Sens.*, vol. 60, 2022, Art. no. 5621414, doi: 10.1109/TGRS.2022.3165817.

[12] W. Shi, Z. Miao, and J. Debayle, "An integrated method for urban main-road centerline extraction from optical remotely sensed imagery," *IEEE Trans. Geosci. Remote Sens.*, vol. 52, no. 6, pp. 3359–3372, Jun. 2014, doi: 10.1109/TGRS.2013.2272593.

[13] Y. Yu, J. Li, H. Guan, F. Jia, and C. Wang, "Learning hierarchical features for automated extraction of road markings from 3-D mobile LiDAR point clouds," *IEEE J. Sel. Topics Appl. Earth Observ. Remote Sens.*, vol. 8, no. 2, pp. 709–726, Feb. 2015, doi: 10.1109/JSTARS.2014.2347276.

[14] R. Alshehhi and P. R. Marpu, "Hierarchical graph-based segmentation for extracting road networks from high-resolution satellite images," *ISPRS J. Photogramm. Remote Sens.*, vol. 126, pp. 245–260, Apr. 2017, doi: 10.1016/j.isprsjprs.2017.02.008.

[15] R. Li and F. Cao, "Road network extraction from high-resolution remote sensing image using homogenous property and shape feature," *J. Indian Soc. Remote Sens.*, vol. 46, no. 5, pp. 1–8, May 2017, doi: 10.1007/s12524-017-0678-6.

[16] Y. Wei, Z. Wang, and M. Xu, "Road structure refined CNN for road extraction in aerial image," *IEEE Geosci. Remote Sens. Lett.*, vol. 14, no. 5, pp. 709–713, May 2017, doi: 10.1109/LGRS.2017.2672734.

[17] H. Zhou, H. Kong, L. Wei, D. Creighton, and S. Nahavandi, "On detecting road regions in a single UAV image," *IEEE Trans. Intell. Transp. Syst.*, vol. 18, no. 7, pp. 1713–1722, Jul. 2017, doi: 10.1109/TITS.2016.2622280.

[18] J. Dai et al., "Development and prospect of road extraction method for optical remote sensing image," *Nat. Remote Sens. Bull.*, vol. 24, no. 7, pp. 804–823, Jul. 2020.

[19] R. Lian, W. Wang, N. Mustafa, and L. Huang, "Road extraction methods in high-resolution remote sensing images: A comprehensive review," *IEEE J. Sel. Topics Appl. Earth Observ. Remote Sens.*, vol. 13, pp. 5489–5507, 2020, doi: 10.1109/JSTARS.2020.3023549.

[20] C. Toth and G. Jóźków, "Remote sensing platforms and sensors: A survey," *ISPRS J. Photogramm. Remote Sens.*, vol. 115, pp. 22–36, Nov. 2015, doi: 10.1016/j.isprsjprs.2015.10.004.

[21] R. Lian, Z. Zhang, C. Zou, and L. Huang, "An effective road centerline extraction method from VHR," *IEEE Geosci. Remote Sens. Lett.*, vol. 19, 2022, Art. no. 6509205, doi: 10.1109/LGRS.2022.3170307.

[22] Y. Xu, Z. Xie, Y. Feng, and Z. Chen, "Road extraction from high-resolution remote sensing imagery using deep learning," *Remote Sens.*, vol. 10, no. 9, Sep. 2018, Art. no. 1461, doi: 10.3390/rs10091461.

[23] L. Shanmugam and V. Kaliaperumal, "Junction-aware water flow approach for urban road network extraction," *IET Image Process.*, vol. 10, no. 3, pp. 227–234, Mar. 2016, doi: 10.1049/iet-ipr.2015.0263.

[24] M. O. Sghaier and R. Lepage, "Road extraction from very high resolution remote sensing optical images based on texture analysis and beamlet transform," *IEEE J. Sel. Topics Appl. Earth Observ. Remote Sens.*, vol. 9, no. 5, pp. 1946–1958, May 2016, doi: 10.1109/JSTARS.2015.2449296.

[25] F. Saba, M. J. V. Zoej, and M. Mokhtarzade, "Optimization of multiresolution segmentation for object-oriented road detection from high-resolution images," *Can. J. Remote Sens.*, vol. 42, no. 2, pp. 75–84, Mar. 2016, doi: 10.1080/07038992.2016.1160770.

[26] T. Zhou, C. Sun, and H. Fu, "Road information extraction from high-resolution remote sensing images based on road reconstruction," *Remote Sens.*, vol. 11, no. 1, Jan. 2019, Art. no. 79, doi: 10.3390/rs11010079.

[27] J. Wang, Q. Qin, Z. Gao, J. Zhao, and X. Ye, "A new approach to urban road extraction using high-resolution aerial image," *ISPRS Int. J. Geo-Inf.*, vol. 5, no. 7, Jul. 2016, Art. no. 114, doi: 10.3390/ijgi5070114.

[28] Y. Wei, K. Zhang, and S. Ji, "Simultaneous road surface and centerline extraction from large-scale remote sensing images using CNN-based segmentation and tracing," *IEEE Trans. Geosci. Remote Sens.*, vol. 58, no. 12, pp. 8919–8931, Dec. 2020, doi: 10.1109/TGRS.2020.2991733.

[29] P. Li et al., "Exploring label probability sequence to robustly learn deep convolutional neural networks for road extraction with noisy datasets," *IEEE Trans. Geosci. Remote Sens.*, vol. 60, 2022, Art. no. 5614018, doi: 10.1109/TGRS.2021.3128539.

[30] X. Zhang, W. Ma, C. Li, J. Wu, X. Tang, and L. Jiao, "Fully convolutional network-based ensemble method for road extraction from aerial images," *IEEE Geosci. Remote Sens. Lett.*, vol. 17, no. 10, pp. 1777–1781, Oct. 2020, doi: 10.1109/LGRS.2019.2953523.

[31] X. Zhang, X. Han, C. Li, X. Tang, H. Zhou, and L. Jiao, "Aerial image road extraction based on an improved generative adversarial network," *Remote Sens.*, vol. 11, Apr. 2019, Art. no. 930, doi: 10.3390/rs11080930.

[32] S. Shao, L. Xiao, L. Lin, C. Ren, and J. Tian, "Road extraction convolutional neural network with embedded attention mechanism for remote sensing imagery," *Remote Sens.*, vol. 14, Apr. 2022, Art. no. 2061, doi: 10.3390/rs14092061.

[33] D. Liu, J. Zhang, K. Liu, and Y. Zhang, "Aerial remote sensing image cascaded road detection network based on edge sensing module and attention module," *IEEE Geosci. Remote Sens. Lett.*, vol. 19, 2022, Art. no. 6513605, doi: 10.1109/LGRS.2022.3190495.

[34] X. Chen, Q. Sun, W. Guo, C. Qiu, and A. Yu, "GA-Net: A geometry prior assisted neural network for road extraction," *Int. J. Appl. Earth Observ.*, vol. 114, Nov. 2022, Art. no. 103004, doi: 10.1016/j.jag.2022.103004.

[35] Z. Sun, W. Zhou, C. Ding, and M. Xia, "Multi-resolution transformer network for building and road segmentation of remote sensing image," *ISPRS Int. J. Geo-Inf.*, vol. 11, Feb. 2022, Art. no. 165, doi: 10.3390/ijgi11030165.

[36] W. Chen, G. Zhou, Z. Liu, X. Li, X. Zheng, and L. Wang, "NIGAN: A framework for mountain road extraction integrating remote sensing road-scene neighborhood probability enhancements and improved conditional generative adversarial network," *IEEE Trans. Geosci. Remote Sens.*, vol. 60, 2022, Art. no. 5626115, doi: 10.1109/TGRS.2022.3188908.

[37] D. He, Q. Shi, X. Liu, Y. Zhong, G. Xia, and L. Zhang, "Generating annual high resolution land cover products for 28 metropolises in China based on a deep super-resolution mapping network using Landsat imagery GISci," *Remote Sens.*, vol. 59, no. 1, pp. 2036–2067, Nov. 2022, doi: 10.1080/15481603.2022.2142727.

[38] D. He, Q. Shi, X. Liu, Y. Zhong, and X. Zhang, "Deep subpixel mapping based on semantic information modulated network for urban land use mapping," *IEEE Trans. Geosci. Remote Sens.*, vol. 59, no. 12, pp. 10628–10646, Dec. 2021, doi: 10.1109/TGRS.2021.3050824.
[39] G. L. Oliveira, W. Burgard, and T. Brox, "Efficient deep models for monocular road segmentation," in *Proc. IEEE/RSJ Int. Conf. Intell. Robots Syst.*, 2016, pp. 4885–4891, doi: 10.1109/iros.2016.7759717.
[40] B. Dan, M. Will, and P. Ingmar, "Find your own way: Weakly-supervised segmentation of path proposals for urban autonomy," in *Proc. IEEE Int. Conf. Robot. Automat.*, 2017, pp. 204–210, doi: 10.1109/icra.2017.7989025.
[41] W. V. Gansbeke, B. D. Brabandere, D. Neven, M. Proesmans, and L. V. Gool, "End-to-end lane detection through differentiable least-squares fitting," in *Proc. Int. Conf. Comput. Vis. Workshop*, Sep. 2019, pp. 905–913.
[42] H. Zhou, H. Zhang, K. Hasith, and H. Wang, "Real-time robust multi-lane detection and tracking in challenging urban scenarios," in *Proc. IEEE 4th Int. Conf. Adv. Robot. Mechatron.*, 2020, pp. 936–941.
[43] W. Kong, T. Zhong, X. Mai, S. Zhang, M. Chen, and G. Lv, "Automatic detection and assessment of pavement marking defects with street view imagery at the city scale," *Remote Sens.*, vol. 12, Aug. 2022, Art. no. 4037, doi: 10.3390/rs14164037.
[44] Y. Tian et al., "Lane marking detection via deep convolutional neural network," *Neurocomputing*, vol. 280, pp. 46–55, Mar. 2018, doi: 10.1016/j.neucom.2017.09.098.
[45] T. Chen, Z. Chen, Q. Shi, and X. Huang, "Road marking detection and classification using machine learning algorithms," in *Proc. IEEE Intell. Veh. Symp.*, 2015, pp. 617–621, doi: 10.1109/IVS.2015.7225753.
[46] J. H. Yoo, S.-W. Lee, S.-K. Park, and D. H. Kim, "A robust lane detection method based on vanishing point estimation using the relevance of line segments," *IEEE Trans. Intell. Transp. Syst.*, vol. 18, no. 12, pp. 3254–3266, Dec. 2017, doi: 10.1109/TITS.2017.2679222.
[47] U. Ozgunalp, R. Fan, X. Ai, and N. Dahnoun, "Multiple lane detection algorithm based on novel dense vanishing point estimation," *IEEE Trans. Intell. Transp. Syst.*, vol. 18, no. 3, pp. 621–632, Mar. 2017, doi: 10.1109/TITS.2016.2586187.
[48] H. Jung, J. Min, and J. Kim, "An efficient lane detection algorithm for lane departure detection," in *Proc. IEEE Intell. Veh. Symp.*, 2013, pp. 976–981, doi: 10.1109/IVS.2013.6629593.
[49] J. Guo, Z. Wei, and D. Miao, "Lane detection method based on improved RANSAC algorithm," in *Proc. IEEE 12th Int. Symp. Auton. Decentralized Syst.*, 2015, pp. 285–288, doi: 10.1109/ISADS.2015.24.
[50] X. Li, J. Li, X. Hu, and J. Yang, "Line-CNN: End-to-end traffic line detection with line proposal unit," *IEEE Trans. Intell. Transp. Syst.*, vol. 21, no. 1, pp. 248–258, Jan. 2020, doi: 10.1109/TITS.2019.2890870.
[51] M. Herb, T. Weiherer, N. Navab, and F. Tombari, "Lightweight semantic mesh mapping for autonomous vehicles," in *Proc. IEEE Int. Conf. Robot. Automat.*, 2021, pp. 6732–3738, doi: 10.1109/ICRA48506.2021.9560996.
[52] Z. Qin, H. Wang, and X. Li, "Ultra fast structure-aware deep lane detection," in *Proc. Eur. Conf. Comput. Vis.*, Nov. 2020, pp. 276–291, doi: 10.1007/978-3-030-58586-0_7.
[53] S. Yoo et al., "End-to-end lane marker detection via row-wise classification," in *Proc. IEEE/CVF Conf. Comput. Vis. Pattern Recognit. Workshops*, 2020, pp. 4335–4343, doi: 10.1109/CVPRW50498.2020.00511.
[54] L. Tabelini, R. Berriel, T. M. Paixão, C. Badue, A. F. De Souza, and T. Oliveira-Santos, "Keep your eyes on the lane: Real-time attention-guided lane detection," in *Proc. IEEE/CVF Conf. Comput. Vis. Pattern Recognit.*, 2021, pp. 294–302, doi: 10.1109/CVPR46437.2021.00036.
[55] T. Qin, Y. Zheng, T. Chen, Y. Chen, and Q. Su, "RoadMap: A light-weight semantic map for visual localization towards autonomous driving," in *Proc. Conf. Comput. Vis. Pattern Recognit.*, Jun. 2021.
[56] J. Shi, G. Li, L. Zhou, and G. Lv, "Lane-level road network construction based on street-view images," *IEEE J. Sel. Topics Appl. Earth Observ. Remote Sens.*, vol. 15, pp. 4744–4754, 2022, doi: 10.1109/JSTARS.2022.3181464.
[57] J. R. Meijer, M. A. J. Huijbregts, K. C. G. J. Schotten, and A. M. Schipper, "Global patterns of current and future road infrastructure," *Environ. Res. Lett.*, vol. 13, no. 6, May 2018, Art. no. 064006, doi: 10.1088/1748-9326/aabd42.
[58] M. Goodchild, "NeoGeography and the nature of geographic expertise," *J. Location Serv.*, vol. 3, no. 2, pp. 82–96, Aug. 2009, doi: 10.1080/17489720902950374.
[59] M. Haklay, "How good is volunteered geographical information? A comparative study of OpenStreetMap and ordnance survey datasets," *Environ. Plan. B: Plan. Des.*, vol. 37, no. 4, pp. 682–703, Aug. 2010, doi: 10.1068/b35097.
[60] Y. Zhang, X. Li, A. Wang, T. Bao, and S. Tian, "Density and diversity of OpenStreetMap road networks in China," *J. Urban Manage.*, vol. 4, no. 2, pp. 135–146, Dec. 2015, doi: 10.1016/j.jum.2015.10.001.
[61] M. Jendryke, S. C. McClure, T. Balz, and M. Liao, "Monitoring the built-up environment of shanghai on the street-block level using SAR and volunteered geographic information," *Int. J. Digit. Earth*, vol. 10, no. 7, pp. 675–686, Aug. 2016, doi: 10.1080/17538947.2016.1216616.
[62] B. Wilson, K. E. Allstadt, and E. M. Thompson, "A near-real-time model for estimating probability of road obstruction due to earthquake-triggered landslides," *Earthq. Spectra*, vol. 37, no. 4, pp. 2400–2418, Oct. 2021, doi: 10.1177/87552930211020022.
[63] C. Stewart, L. Michele, L. Adrian, and A. Sergio, "Deep learning with open data for desert road mapping," *Remote Sens.*, vol. 12, no. 14, Jul. 2020, Art. no. 2274, doi: 10.3390/rs12142274.
[64] C. Sun et al., "Proximity based automatic data annotation for autonomous driving," *IEEE/CAA J. Automatica Sinica*, vol. 7, no. 2, pp. 395–404, Mar. 2020, doi: 10.1109/JAS.2020.1003033.
[65] R. Dong, Y. Zhang, and J. Zhao, "How green are the streets within the sixth ring road of Beijing—An analysis based on Tencent street view pictures and the green view index," *Int. J. Environ. Res. Public Health*, vol. 15, no. 7, pp. 1367–1389, Jul. 2018, doi: 10.3390/ijerph15071367.
[66] C. Yang et al., "Approach to quantify spatial comfort of urban roads based on street view images," *J. Geo-Inf. Sci.*, vol. 23, no. 5, pp. 785–801, May 2021, doi: 10.12082/dqxxkx.2021.200353.
[67] A. Meyer, N. O. Salscheider, P. F. Orzechowski, and C. Stiller, "Deep semantic lane segmentation for mapless driving," in *Proc. IEEE/RSJ Int. Conf. Intell. Robots Syst.*, 2018, pp. 869–875.
[68] K. He, G. Gkioxari, P. Dollár, and R. Girshick, "Mask R-CNN," *IEEE Trans. Pattern Anal. Mach. Intell.*, vol. 42, no. 2, pp. 386–397, Feb. 2020, doi: 10.1109/TPAMI.2018.2844175.
[69] J. Dai, T. Zhu, Y. Zhang, R. Ma, and W. Li, "Lane-level road extraction from high-resolution optical satellite images," *Remote Sens.*, vol. 11, no. 22, Nov. 2019, Art. no. 2672, doi: 10.3390/rs11222672.
[70] M. Yadav, A. K. Singh, and B. Lohani, "Extraction of road surface from mobile LiDAR data of complex road environment," *Int. J. Remote Sens.*, vol. 38, no. 16, pp. 4645–4672, May 2017, doi: 10.1080/01431161.2017.1320451.
[71] D. Rato and V. Santos, "LIDAR based detection of road boundaries using the density of accumulated point clouds and their gradients," *Robot. Auton. Syst.*, vol. 138, Apr. 2021, Art. no. 103714, doi: 10.1016/j.robot.2020.103714.
[72] L. Liu, Z. Yang, G. Li, K. Wang, T. Chen, and L. Lin, "Aerial images meet crowdsourced trajectories: A new approach to robust road extraction," *IEEE Trans. Neural Netw. Learn. Syst.*, vol. 34, no. 7, pp. 3308–3322, Jul. 202l, doi: 10.1109/TNNLS.2022.3141821.
[73] W. Yang, T. Ai, and W. Lu, "A method for extracting road boundary information from crowdsourcing vehicle GPS trajectories," *Sensor*, vol. 18, no. 4, pp. 1261–1283, Apr. 2018, doi: 10.3390/s18041261.
[74] C. Yang, L. Jiang, X. Chen, C. Wang, and M. Zhao, "Classification and expression of urban topographic features for DEM construction," *J. Geo-Inf. Sci.*, vol. 19, no. 3, pp. 317–325, Mar. 2017, doi: 10.3724/SP.J.1047.2017.00317.
[75] P. Li et al., "Exploring multiple crowdsourced data to learn deep convolutional neural networks for road extraction," *Int. J. Appl. Earth Observ.*, vol. 14, Dec. 2021, Art. no. 102954, doi: 10.1016/j.jag.2021.102544.

Cancan Yang received the B.S. degree in remote sensing science and technology from the Henan Polytechnic University, Henan, China, in 2011, and the M.S. degree in surveying and mapping engineering from the Henan Polytechnic University, in 2013. She is currently working toward the Ph.D. degree in forest management with the School of Beijing Forestry University, Beijing, China.

She is currently working as a Teacher with the School of Geographic Information and Tourism, Chuzhou University, Chuzhou, China. Her research interests include urban terrain analysis, urban information extraction, remote sensing applications, and forestry remote sensing.

Ling Jiang received the B.S. degree in geographic information science from the Hunan University of Science and Technology, Xiangtan, China, in 2009, and the Ph.D. degree in cartography and geographic information system from the Nanjing Normal University, Nanjing, China, in 2014.

He is currently a Professor of geographic information science with the Chuzhou University, Chuzhou, China. His research interests include digital terrain analysis, urban remote sensing applications, and high-performance geocomputing.

Wen Dai received the B.S. degree in surveying and mapping engineering from the Guizhou University, Guizhou, China, in 2016, and the Ph.D. degree in cartography and geographic information systems from the Nanjing Normal University, Nanjing, China, in 2021.

During the Ph.D. degree, he was cotrained with the Université de Lausanne, Écublens, Switzerland, for 1 year. He is currently a Teacher with the Nanjing University of Information Science and Technology, Nanjing, China. His research interests include remote sensing image analysis and digital terrain analysis.

Dr. Dai is a Reviewer of international journals, such as *GIScience & Remote Sensing* and the *International Journal of Applied Earth Observation and Geoinformation.*

Daoli Peng received the M.S. and Ph.D. degrees in forest management from the Beijing Forestry University, Beijing, China, in 1988 and 1994, respectively.

He is currently a Professor with the Beijing Forestry University. He has authored/coauthored more than 100 research articles in international journals, such as *Science of the Total Environment, Ecological Indicators, Catena and Forest Ecology and Management.* His research interests include forest resource monitoring and evaluation, remote sensing, and information technology.

Kai Deng received the B.S. degree in geographic information systems from the Jiangxi University of Science and Technology, Jiangxi, China, in 2010, and the M.S. degree in cartography and geographic information systems from the Jiangxi University of Science and Technology, in 2013.

He is currently working as a Teacher with the School of Geographic Information and Tourism, Chuzhou University, Chuzhou, China. His research interests include GIS Big Data analysis and information extraction.

Mingwei Zhao received the B.S. degree in cartography and geographic information system from the Nanjing Normal University, Jiangsu, China, in 2012, and the Ph.D. degree in cartography and geographic information system from the Institute of Geographic Sciences and Natural Resources Research, CAS, Beijing, China, in 2015.

He is currently an Associate Professor with the School of Geographic Information and Tourism, Chuzhou University, Chuzhou, China. His research interests include urban terrain analysis, urban information extraction, and remote sensing applications.

Xiaoli Huang received the B.S. degree in geographic science from the Lanzhou University, Lanzhou, China, in 2013, and the Ph.D. degree in cartography and geographical information system from the Nanjing Normal University, Nanjing, China, in 2019.

He is currently working as a Teacher with the School of Geographic Information and Tourism, Chuzhou University, Chuzhou, China. His research interests include digital terrain analysis, geomorphometry, and object-oriented image analysis.

Xi Chen received the B.S. degree in geography from the Anqing Normal University, Anhui, China, in 2016, the M.S. and D.S. degrees in physical geography from the Nanjing Normal University, Nanjing, China, in 2021, and the Ph.D. degree in geography from the Nanjing Normal University, Nanjing, China, in 2021.

He is currently working as a Teacher with the School of Geographic Information and Tourism, Chuzhou University, Chuzhou, China. His research interests include material cycle in basin and city, LUCC, and remote sensing applications.